

# Supplementary Information for “A New Interpretation of the Structure and Solvent Dependence of the Far UV Circular Dichroism Spectrum of Short Oligopeptides”

*Anshuman Kumar,<sup>a</sup> Reinhard Schweitzer-Stenner,<sup>\*b</sup> and Bryan M. Wong<sup>\*a</sup>*

<sup>a</sup>Department of Chemical & Environmental Engineering and Materials Science & Engineering Program, University of California-Riverside, Riverside, CA 92521, United States

<sup>b</sup>Department of Chemistry, Drexel University, Philadelphia, PA 19104, United States

\*Corresponding authors. E-mail: [rs344@drexel.edu](mailto:rs344@drexel.edu). Web: <http://www.schweitzer-stenner.com>

E-mail: [bryan.wong@ucr.edu](mailto:bryan.wong@ucr.edu). Web: <http://www.bmwong-group.com>

## Contents

**p. S3, Figure S1:** ECD spectra of explicitly-solvated GAG in the optimized pPII conformation calculated with different range-separation values of  $\omega = 0.20$  and  $0.25$

**p. S4, Figure S2:** ECD spectra of explicitly-solvated GAG in the optimized pPII conformation calculated with different exchange-correlation functionals

**p. S5, Figure S3:** ECD spectra of explicitly-solvated GAG in the optimized  $\beta$ -strand conformation calculated with different basis sets

**p. S6, Figure S4:** ECD spectra of explicitly-solvated GAG in the optimized pPII conformation with different configurations of explicit water molecules

**p. S7, Figure S5:** Optimized geometry of GAG in the pPII conformation at the  $\omega$ B97XD/cc-pVTZ level of theory in implicit and explicit water; **Figure S6:** Absorption spectra of GAG in the pPII conformation calculated at the  $\omega$ B97XD/cc-pVTZ level of theory in implicit and explicit water

**p. S8, Figure S7:** Optimized geometry of GAG in the  $\beta$  conformation at the  $\omega$ B97XD/cc-pVTZ level of theory in implicit and explicit water; **Figure S8:** Absorption spectra of GAG in the  $\beta$  conformation calculated at the  $\omega$ B97XD/cc-pVTZ level of theory in implicit and explicit water

**p. S9, Figure S9:** Natural transition orbitals (NTOs) and hole/particle pairs of GAG in the pPII conformation with explicit water for the first and fourth transitions

**p. S10, Figure S10:** Natural transition orbitals (NTOs) and hole/particle pairs of GAG in the pPII conformation with implicit water for the second, fifth, and sixth transitions

**p. S11, Figure S11:** Natural transition orbitals (NTOs) and hole/particle pairs of GAG in the  $\beta$  conformation with implicit water for the first and fourth transitions

**p. S12, Figure S12:** Natural transition orbitals (NTOs) and hole/particle pairs of GAG in the  $\beta$  conformation with explicit water for the first and fourth transitions

**p. S13, Table S1:** Dihedral angles of GAG in the pPII and  $\beta$  conformations calculated at the  $\omega$ B97XD/cc-pVTZ level of theory in implicit water and explicit water; **Table S2:** List of the first five excited states for GAG in the pPII conformation calculated at the  $\omega$ B97XD/cc-pVTZ level of theory in implicit water and explicit water

**p. S14, Table S3:** List of the first five excited states for GAG in the  $\beta$  conformation calculated at the  $\omega$ B97XD/cc-pVTZ level of theory in implicit water and explicit water

**p. S15,** Computational Details

**p. S16,** References

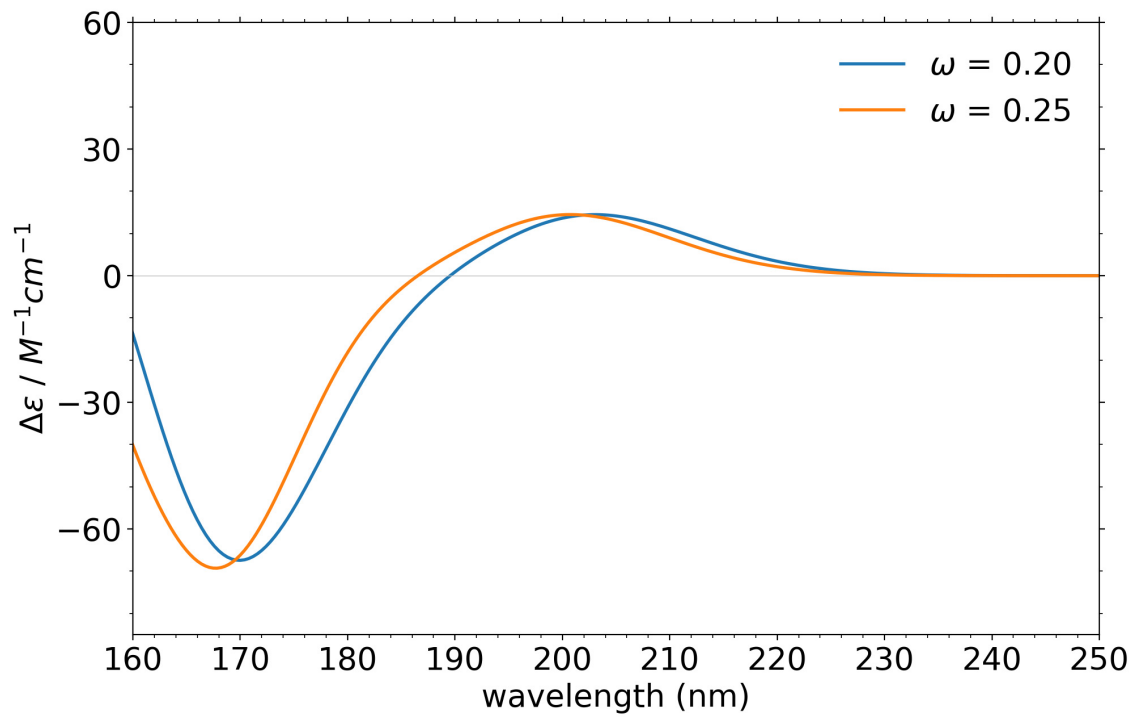


**Figure S1.** ECD spectra of explicitly-solvated GAG in the optimized pPII conformation calculated with different range-separation values of  $\omega = 0.20$  and  $0.25$ .

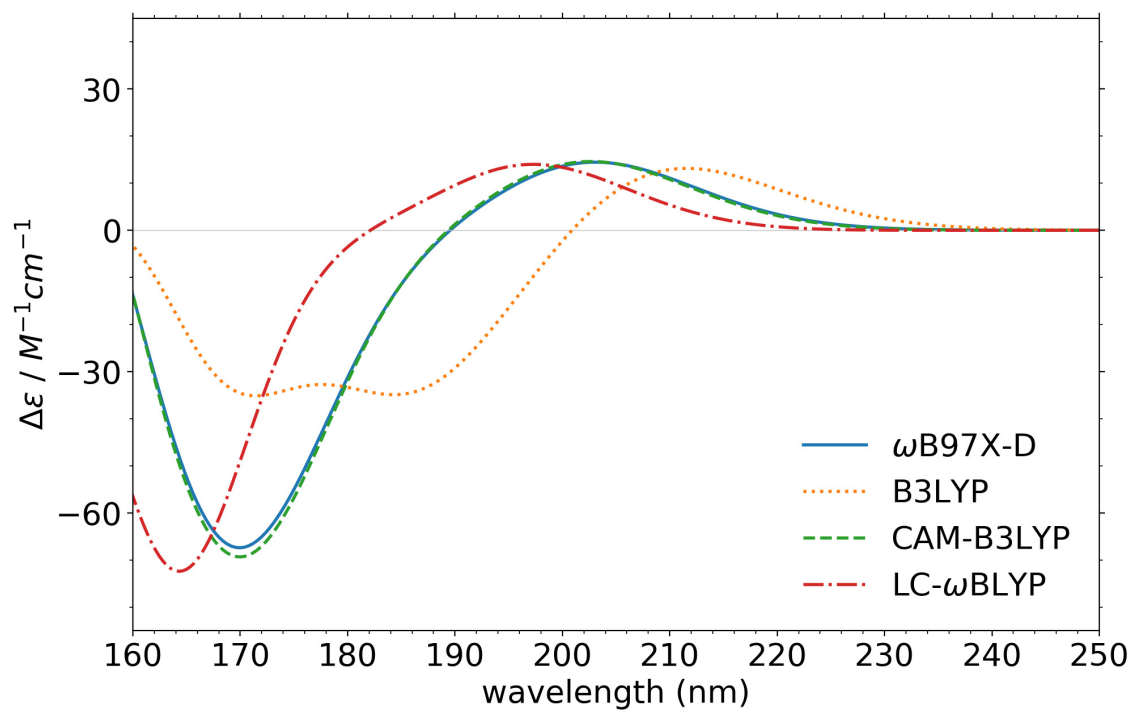


**Figure S2** ECD spectra of explicitly-solvated GAG in the optimized pPII conformation calculated with different exchange-correlation functionals.

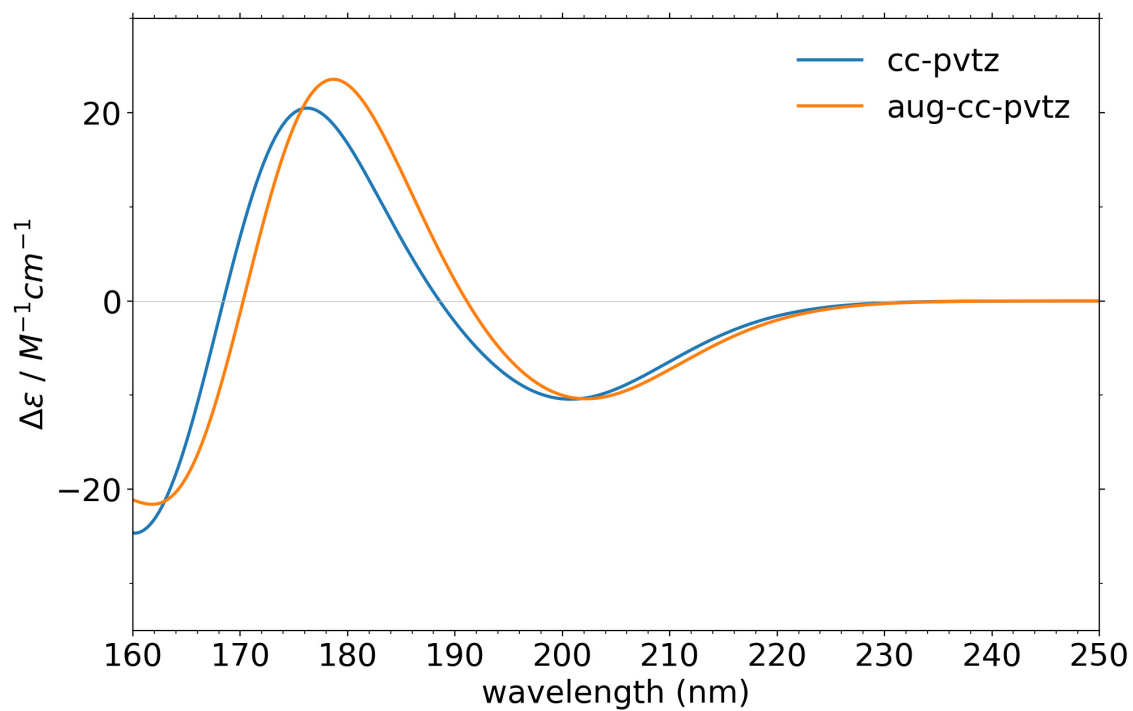


**Figure S3.** ECD spectra of explicitly-solvated GAG in the optimized  $\beta$ -strand conformation calculated with different basis sets.

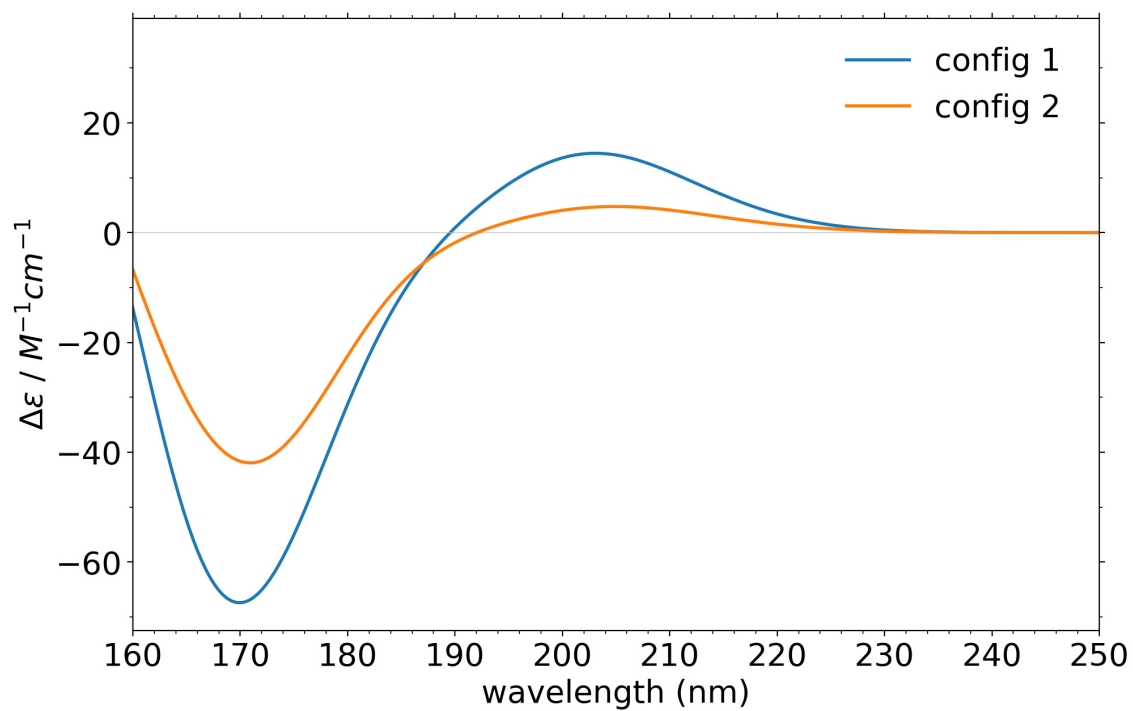


**Figure S4.** ECD spectra of explicitly-solvated GAG in the optimized pPII conformation with different configurations of explicit water molecules.

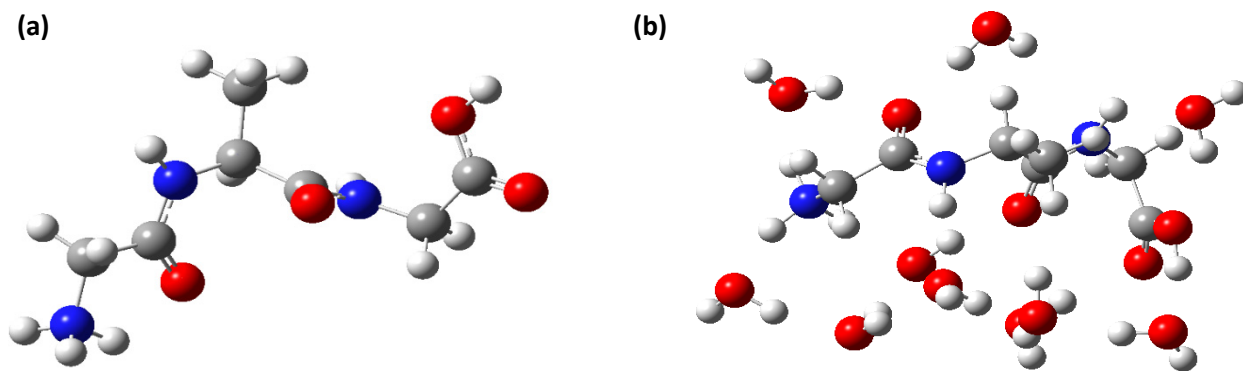


**Figure S5.** Optimized geometry of GAG in the pII conformation at the  $\omega$ B97XD/cc-pVTZ level of theory in (a) implicit and (b) explicit water.

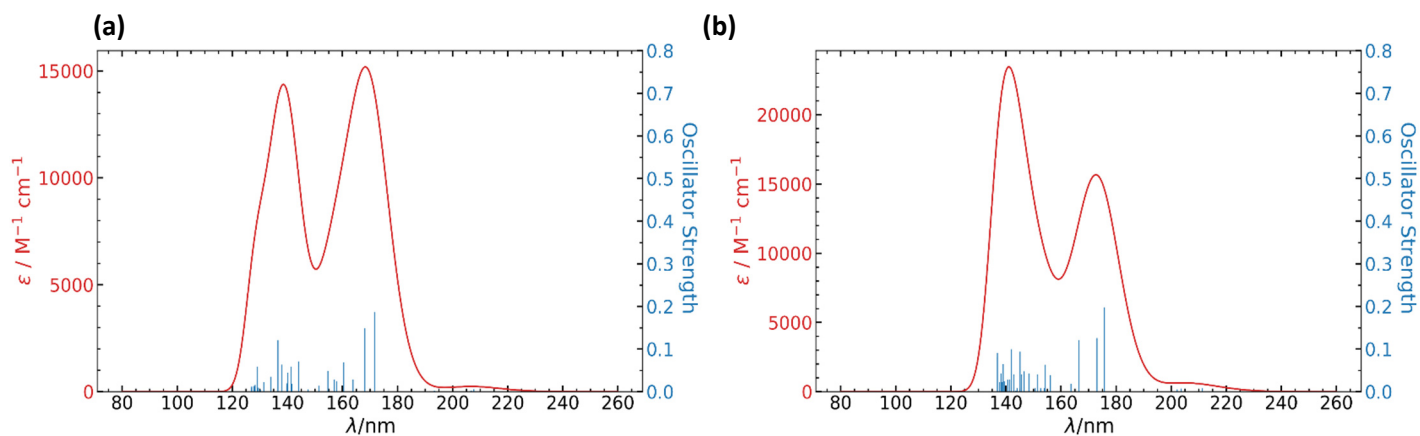


**Figure S6.** Absorption spectra of GAG in the pII conformation calculated at the  $\omega$ B97XD/cc-pVTZ level of theory in (a) implicit and (b) explicit water.

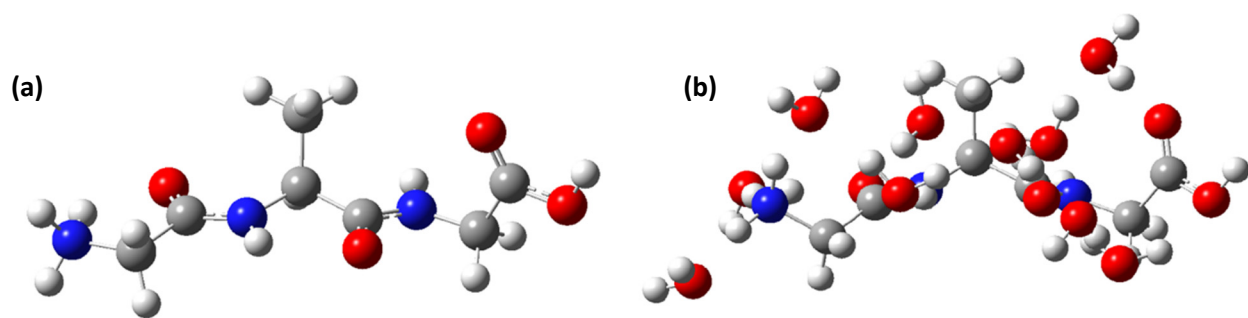


**Figure S7.** Optimized geometry of GAG in the  $\beta$  conformation at the  $\omega$ B97XD/cc-pVTZ level of theory in (a) implicit and (b) explicit water.

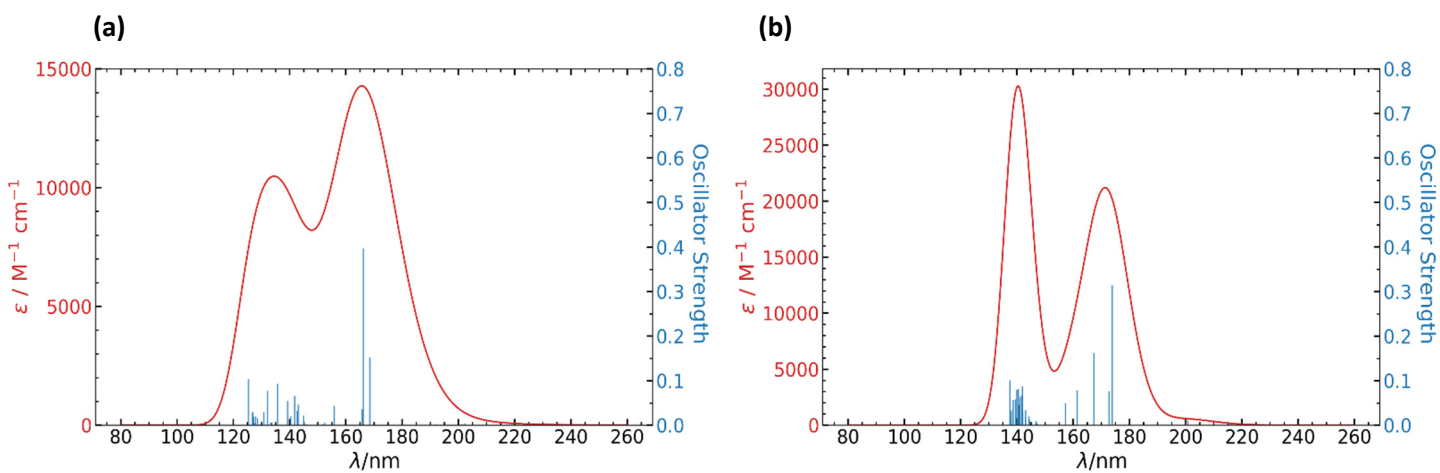
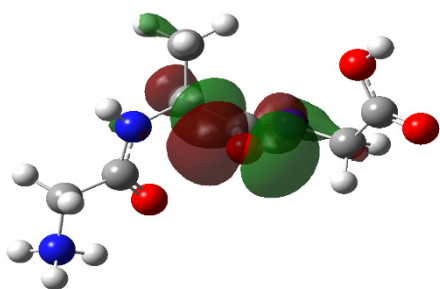
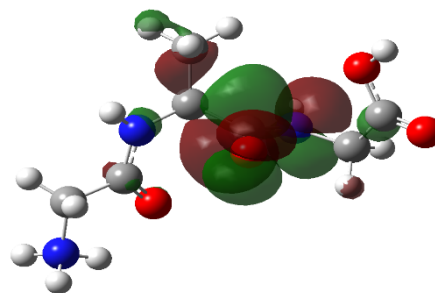


**Figure S8.** Absorption spectra of GAG in the  $\beta$  conformation calculated at the  $\omega$ B97XD/cc-pVTZ level of theory in (a) implicit and (b) explicit water.

(a) |1>       $w = 0.99$     $\omega = 5.97$  eV    $f = 0.004$

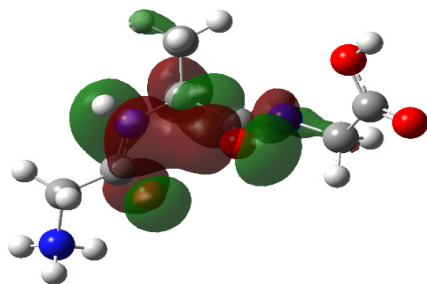


Hole

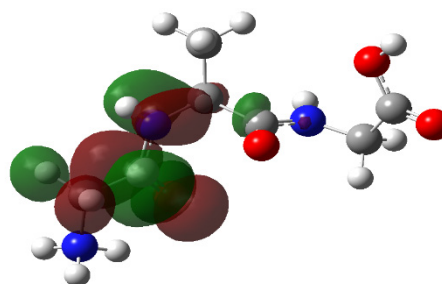


Particle

(b) |4>       $w = 0.93$     $\omega = 7.22$  eV    $f = 0.19$



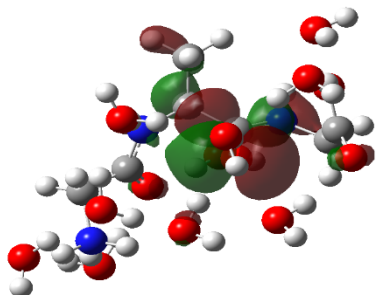
Hole



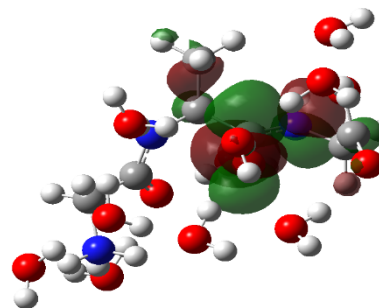
Particle

**Figure S9.** Natural transition orbitals<sup>1</sup> (NTOs) of GAG in the pPII conformation with implicit water obtained from calculations at the  $\omega$ B97XD/cc-pVTZ level of theory. Hole and particle pairs for (a) the first transition corresponding to the positive peak in the ECD spectra at around 202 nm and (b) the fourth transition corresponding to the negative peak at around 172 nm. Panels give the excited state number, associated eigenvalue ( $w$ ), transition energy ( $\omega$ ), and oscillator strength ( $f$ ).

(a) |2>  $w = 0.97$   $\omega = 6.09$  eV  $f = 0.006$

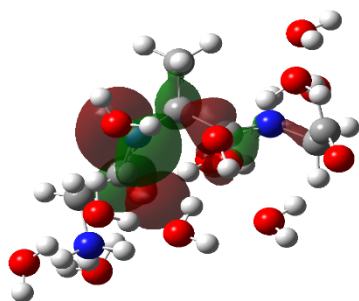


Hole

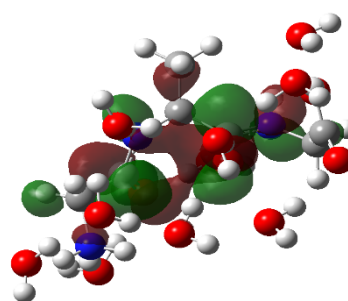


Particle

(b) |5>  $w = 0.90$   $\omega = 7.16$  eV  $f = 0.12$

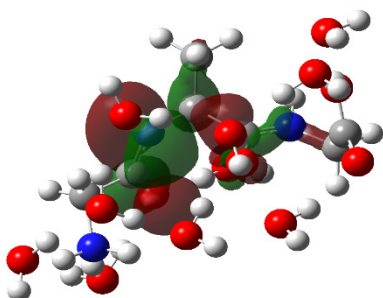


Hole

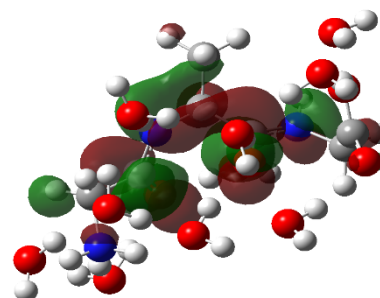


Particle

(c) |6>  $w = 0.88$   $\omega = 7.45$  eV  $f = 0.12$



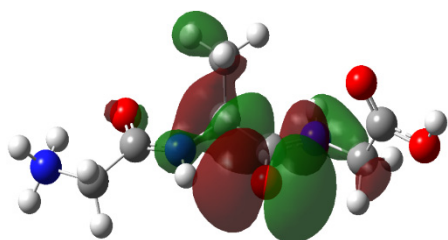
Hole



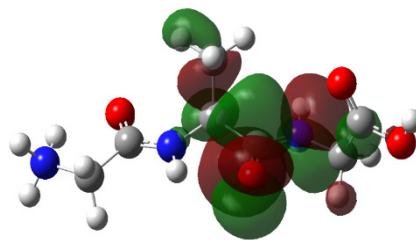
Particle

**Figure S10.** Natural transition orbitals (NTOs) of GAG in the pPII conformation with explicit water obtained from calculations at the  $\omega$ B97XD/cc-pVTZ level of theory. Hole and particle pairs for (a) the second transition corresponding to the positive peak in the ECD spectra at around 205 nm (b) the fifth transition corresponding to the negative peak at around 174 nm and (c) the sixth transition corresponding to the negative peak at around 166 nm. Panels give the excited state number, associated eigenvalue ( $w$ ), transition energy ( $\omega$ ), and oscillator strength ( $f$ ).

(a) |1>       $w = 0.99$     $\omega = 6.13$  eV    $f = 0.003$

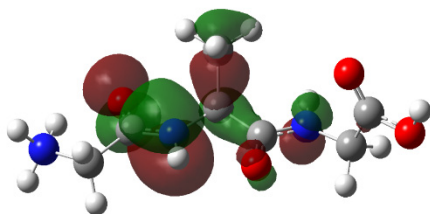


Hole

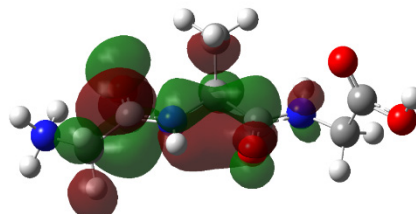


Particle

(b) |4>       $w = 0.92$     $\omega = 7.35$  eV    $f = 0.15$



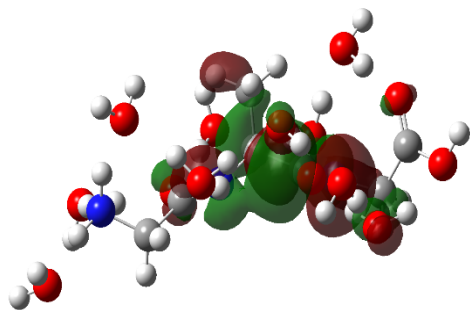
Hole



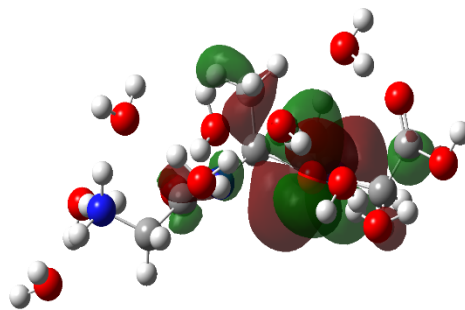
Particle

**Figure S11.** Natural transition orbitals (NTOs) of GAG in the  $\beta$  conformation with implicit water obtained from calculations at the  $\omega$ B97XD/cc-pVTZ level of theory. Hole and particle pairs for (a) the first transition corresponding to the positive peak in the ECD spectra at around 204 nm and (b) the fourth transition corresponding to the positive peak at around 170 nm. Panels give the excited state number, associated eigenvalue ( $w$ ), transition energy ( $\omega$ ), and oscillator strength ( $f$ ).

(a) |1>  $w = 0.87$   $\omega = 6.18$  eV  $f = 0.01$

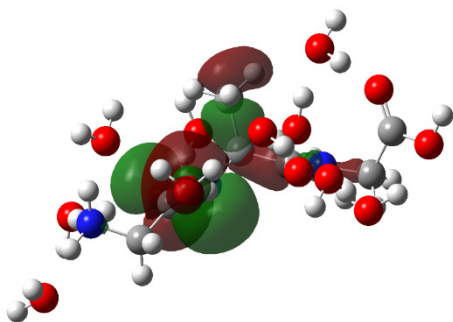


Hole

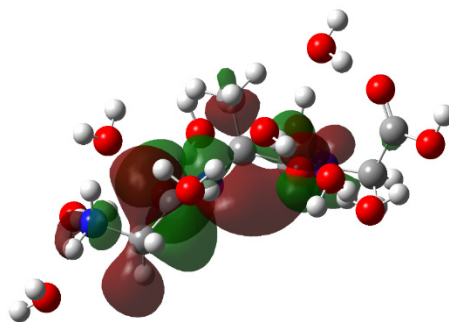


Particle

(b) |4>  $w = 0.91$   $\omega = 7.13$  eV  $f = 0.31$



Hole



Particle

**Figure S12.** Natural transition orbitals (NTOs) of GAG in the  $\beta$  conformation with explicit water obtained from calculations at the  $\omega$ B97XD/cc-pVTZ level of theory. Hole and particle pairs for (a) the first transition corresponding to the negative peak in the ECD spectra at around 202nm and (b) the fourth transition corresponding to the positive peak at around 178 nm. Panels give the excited state number, associated eigenvalue ( $w$ ), transition energy ( $\omega$ ), and oscillator strength ( $f$ ).

**Table S1.** Dihedral angles of GAG in the pPII and  $\beta$  conformations calculated at the  $\omega$ B97XD/cc-pVTZ level of theory in (a) implicit water and (b) explicit water.

	GAG pPII		GAG $\beta$	
	Implicit water	Explicit Water	Implicit water	Explicit Water
$\phi$	-65.27	-71.93	-160.97	-137.84
$\psi$	149.43	163.59	162.38	131.55

**Table S2.** List of the first five excited states for GAG in the pPII conformation calculated at the  $\omega$ B97XD/cc-pVTZ level of theory in (a) implicit water and (b) explicit water.

(a) Implicit Water

Excited State	$\Delta E^a$ (eV)	$\lambda^b$ (nm)	$f^c$	$R^d$ ( $10^{-40}$ erg.esu.cm/Gauss)
1	5.9693	207.70	0.0043	13.55
2	5.9966	206.76	0.0014	2.65
3	6.4112	193.39	0.0008	10.09
4	7.2200	171.72	0.1854	-68.19
5	7.3729	168.16	0.1471	-21.60

<sup>a</sup>Excitation Energy, <sup>b</sup>Wavelength, <sup>c</sup>Oscillator Strength, and <sup>d</sup>Rotatory Strength (velocity)

(b) Explicit Water

Excited State	$\Delta E^a$ (eV)	$\lambda^b$ (nm)	$f^c$	$R^d$ ( $10^{-40}$ erg.esu.cm/Gauss)
1	5.8687	211.26	0.0064	-1.69
2	6.0906	203.57	0.0060	28.45
3	6.1329	202.16	0.0041	11.51
4	7.0534	175.78	0.1964	-16.09
5	7.1643	173.06	0.1246	-75.68

<sup>a</sup>Excitation Energy, <sup>b</sup>Wavelength, <sup>c</sup>Oscillator Strength, and <sup>d</sup>Rotatory Strength (velocity)

**Table S3.** List of the first five excited states for GAG in the  $\beta$  conformation calculated at the  $\omega$ B97XD/cc-pVTZ level of theory in (a) implicit water and (b) explicit water

(a) Implicit water

Excited State	$\Delta E^a$ (eV)	$\lambda^b$ (nm)	$f^c$	$R^d$ ( $10^{-40}$ erg.esu.cm/Gauss)
1	6.1282	202.32	0.0028	17.34
2	6.1590	201.31	0.0007	0.44
3	6.4477	192.29	0.0008	-5.59
4	7.3592	168.48	0.1512	34.02
5	7.4612	166.17	0.3955	-39.79

<sup>a</sup>Excitation Energy, <sup>b</sup>Wavelength, <sup>c</sup>Oscillator Strength, and <sup>d</sup>Rotatory Strength (velocity)

(b) Explicit water

Excited State	$\Delta E^a$ (eV)	$\lambda^b$ (nm)	$f^c$	$R^d$ ( $10^{-40}$ erg.esu.cm/Gauss)
1	6.1757	200.76	0.0099	-12.60
2	6.1926	200.21	0.0023	-12.52
3	6.1950	200.14	0.0008	-2.63
4	7.1293	173.91	0.3130	77.90
5	7.1766	172.76	0.0749	-17.85

<sup>a</sup>Excitation Energy, <sup>b</sup>Wavelength, <sup>c</sup>Oscillator Strength, and <sup>d</sup>Rotatory Strength (velocity)

## Computational Details

All calculations were performed at 298.15 K with the Gaussian 09 program package (revision E.01)<sup>2</sup> using default algorithms. Density functional theory (DFT) at the  $\omega$ B97XD/cc-pVTZ level of theory<sup>3</sup> was employed to optimize the geometry of the GAG conformers. Previous studies<sup>4</sup> have shown that the range-separated  $\omega$ B97XD functional (which includes dispersion and a range-separated portion of nonlocal exchange) accurately reproduces experimental spectra. The Cartesian coordinates used as initial guesses for the geometry optimization in this paper can be found in the Supporting Information of Ilawe et al.<sup>5</sup> All geometries reported here correspond to local minima of the potential energy surface in the absence of imaginary frequencies. Solvent effects in the implicit solvent model were modeled using the polarizable continuum model (PCM)<sup>6</sup> approach. The specific PCM model used in this work is the implementation devised by Tomasi and co-workers<sup>7</sup> that creates a solute cavity via a set of overlapping spheres to calculate the solvent reaction field.

Time Dependent Density Functional Theory (TD-DFT) at the same level of theory was employed to calculate the excitation energy and rotatory strength  $R_{0\lambda}$ . In the implicit solvent environment, the PCM technique employs a linear response formalism by adding the necessary terms to the excited-state equations (thereby including the solvent effects on the excited states).<sup>8,9</sup> The calculated rotatory strengths were plotted as an electronic circular dichroism (ECD) curve via a summation of Gaussian functions. Rotatory strengths are reported in the usual c.g.s. units of  $10^{-40}$  esu·cm·erg/G, where 1 esu·cm·erg/G corresponds to approximately  $3.336 \times 10^{-15}$  C·m·J/T in SI units. Following previous computational studies<sup>10,11,12</sup> of circular dichroism (CD) spectra, we have used the following relation

$$R_{0\lambda} = 22.97 \int_{\text{CD band } \lambda} \frac{\Delta\epsilon(E)}{E} dE, \quad (1)$$

where  $R_{0\lambda}$  is in  $10^{-40}$  c.g.s. units, the difference in the absorption coefficients for left and right-hand circular polarized light,  $\Delta\epsilon$ , is in 1/(mol·cm), and  $E$  is in eV. For each computed excitation, a normalized Gaussian centered at the corresponding wavelength is scaled to reproduce the computed  $R_{0\lambda}$  by equation (1). The plotted theoretical “CD spectrum” is then obtained as the superposition of all these Gaussian curves. Unless otherwise noted, for the linewidth  $\Delta E$ , we employed the empirical procedure by Brown et al. in Ref. 9, which corresponds to  $\Delta E \approx 0.08\sqrt{E}$  with  $E$  in eV. The linewidths are used here as adjustable parameters in order to mimic a real spectrum.<sup>13</sup> The absorption spectra are simulated by superposing and finally summing each Gaussian at the individual electronic transitions. The width of each Gaussian used in our studies was 0.4 – 0.6 eV.<sup>14</sup> We note here that important corrections to the excitation energy arising from molecular vibrations are currently neglected.

## References

1. Martin, R. L., Natural Transition Orbitals. *J. Chem. Phys.* **2003**, *118*, 4775-4777.
2. Frisch, M. J.; Trucks, G. W.; Schlegel, H. B.; Scuseria, G. E.; Robb, M. A.; Cheeseman, J. R.; Scalmani, G.; Barone, V.; Mennucci, B.; Petersson, G. A.; Nakatsuji, H.; Caricato, M.; Li, X.; Hratchian, H. P.; Izmaylov, A. F.; Bloino, J.; Zheng, G.; Sonnenberg, J. L.; Hada, M.; Ehara, M.; Toyota, K.; Fukuda, R.; Hasegawa, J.; Ishida, M.; Nakajima, T.; Honda, Y.; Kitao, O.; Nakai, H.; Vreven, T.; Montgomery, J. A.; Peralta, J. E.; Ogliaro, F.; Bearpark, M.; Heyd, J. J.; Brothers, E.; Kudin, K. N.; Staroverov, V. N.; Kobayashi, R.; Normand, J.; Raghavachari, K.; Rendell, A.; Burant, J. C.; Iyengar, S. S.; Tomasi, J.; Cossi, M.; Rega, N.; Millam, J. M.; Klene, M.; Knox, J. E.; Cross, J. B.; Bakken, V.; Adamo, C.; Jaramillo, J.; Gomperts, R.; Stratmann, R. E.; Yazyev, O.; Austin, A. J.; Cammi, R.; Pomelli, C.; Ochterski, J. W.; Martin, R. L.; Morokuma, K.; Zakrzewski, V. G.; Voth, G. A.; Salvador, P.; Dannenberg, J. J.; Dapprich, S.; Daniels, A. D.; Farkas, Foresman, J. B.; Ortiz, J. V.; Cioslowski, J.; Fox, D. J., Gaussian 09, Revision B.01. Wallingford CT, 2009.
3. Chai, J.-D.; Head-Gordon, M., Long-Range Corrected Hybrid Density Functionals with Damped Atom-Atom Dispersion Corrections. *Phys. Chem. Chem. Phys.* **2008**, *10*, 6615-6620.
4. Zara, Z.; Iqbal, J.; Ayub, K.; Irfan, M.; Mahmood, A.; Khera, R. A.; Eliasson, B., A Comparative Study of DFT Calculated and Experimental UV/Visible Spectra for Thirty Carboline and Carbazole Based Compounds. *J. Mol. Struct.* **2017**, *1149*, 282-298.
5. Ilawe, N. V.; Raeber, A. E.; Schweitzer-Stenner, R.; Toal, S. E.; Wong, B. M., Assessing Backbone Solvation Effects in the Conformational Propensities of Amino Acid Residues in Unfolded Peptides. *Phys. Chem. Chem. Phys.* **2015**, *17*, 24917-24924.
6. Tomasi, J.; Mennucci, B.; Cammi, R., Quantum Mechanical Continuum Solvation Models. *Chem. Rev.* **2005**, *105*, 2999-3094.
7. Fortunelli, A.; Tomasi, J., The Implementation of Density Functional theory within the Polarizable Continuum Model for Solvation. *Chem. Phys. Lett.* **1994**, *231*, 34-39.
8. Cammi, R.; Mennucci, B.; Tomasi, J., Fast Evaluation of Geometries and Properties of Excited Molecules in Solution: A Tamm-Dancoff Model with Application to 4-Dimethylaminobenzonitrile. *J. Phys. Chem. A* **2000**, *104* (23), 5631-5637.
9. Cossi, M.; Barone, V., Time-Dependent Density Functional Theory for Molecules in Liquid Solutions. *J. Chem. Phys.* **2001**, *115*, 4708-4717.
10. Grimme, S.; Peyerimhoff, S. D.; Bartram, S.; Vögtle, F.; Breest, A.; Hormes, J., Experimental and Theoretical Study of the Circular Dichroism Spectra of Oxa- and Thia- [2.2] Metacyclophane. *Chem. Phys. Lett.* **1993**, *213*, 32-40.
11. Brickell, W. S.; Brown, A.; Kemp, C. M.; Mason, S. F.,  $\pi$ -Electron Absorption and Circular Dichroism Spectra of [6]- and [7]-Helicene. *J. Chem. Soc. A* **1971**, *0*, 756-760.
12. Brown, A.; Kemp, C. M.; Mason, S. F., Electronic Absorption, Polarised Excitation, and Circular Dichroism Spectra of [5]-Helicene (Dibenzo[c,g]phenanthrene). *J. Chem. Soc. A* **1971**, *0*, 751-755.
13. Autschbach, J.; Ziegler, T.; Gisbergen, S. J. A. v.; Baerends, E. J., Chiroptical Properties from Time-Dependent Density Functional Theory. I. Circular Dichroism Spectra of Organic Molecules. *J. Chem. Phys.* **2002**, *116*, 6930-6940.
14. Vitova, T.; Pidchenko, I.; Fellhauer, D.; Bagus, P. S.; Joly, Y.; Pruessmann, T.; Bahl, S.; Gonzalez-Robles, E.; Rothe, J.; Altmaier, M.; Denecke, M. A.; Geckeis, H., The Role of the 5f Valence Orbitals of Early Actinides in Chemical Bonding. *Nat. Commun.* **2017**, *8*, 16053.